ELSEVIER

Marine Geology 242 (2007) 123 – 140

MARINE GEOLOGY
INTERNATIONAL JOURNAL OF MARINE GEOLOGY, GEOCHEMISTRY AND GEOPHYSICS

www.elsevier.com/locate/margeo

# Climate cyclicity in late Holocene anoxic marine sediments from the Seymour–Belize Inlet Complex, British Columbia

R. Timothy Patterson [a,*], Andreas Prokoph [b], Eduard Reinhardt [c], Helen M. Roe [d]

[a] *Department of Earth Sciences and Ottawa-Carleton Geoscience Centre, Carleton University, Ottawa, Ontario, Canada K1S 5B6*
[b] *SPEEDSTAT, 19 Langstrom Crescent, Ottawa, Ontario, Canada K1G 5J5*
[c] *School of Geography and Geology, McMaster University, 1280 Main St W, Hamilton, Ontario, Canada L8S 4K1*
[d] *School of Geography, Archaeology and Palaeoecology, Queen's University of Belfast, Belfast, Northern Ireland, BT7 1NN, UK*

Accepted 4 April 2007

**Abstract**

An 8.72 m late Holocene sediment core (VEC02A07) obtained from Alison Sound in the Belize–Seymour Inlet Complex of central British Columbia, Canada was deposited between ~3500–1000 yr BP under primarily anoxic marine conditions. This core contains a detailed cyclic record of land–sea interactions as evidenced by significant fluctuations in marine primary productivity and changes in the supply of terrigenous material that can be related to long term variation in the relative influence of the Aleutian Low (AL) and North Pacific High (NPH).

Sedimentologically, the core is characterized by alternating intervals of fine-grained massive intervals (70%), laminated intervals (23%), turbidites (5%) and graded silt–clay layers (2%). The laminated intervals are comprised of couplets that vary between light-coloured, diatom-rich layers, deposited primarily during the summer months, and dark-coloured, mineral-rich layers deposited during winter. Laminated couplets are most common in portions of the core deposited between ~3150 and 2700 yr BP, which corresponds to an episode of regional neoglaciation.

Time-series analysis was carried out on high-resolution particle size measurements obtained from core sub-samples and on sediment grey-scale colour variability derived from X-ray scans of the core. Non-linear time-series analyses revealed that the succession of massive and laminated sedimentation displayed characteristics of self-organization following a power law relationship for core length segments of <13 cm (<~50 years of deposition). Wavelet and spectral time-series analysis indicated that core length segments of >13 cm (>~50 years of deposition) contained evidence of sedimentary depositional cycles of ~70–96, 135–155 and 250–330 years that reflect changes in AL and NPH mediated regional precipitation patterns that can in turn be related to larger-scale climate drivers such as the Pacific Decadal Oscillation (PDO) or solar irradiance cyclicity.


*Keywords:* NE Pacific; laminated marine sediments; wavelet transformation; climate cyclicity; image analysis; climate change

## 1. Introduction

The coastal region of British Columbia, Canada is characterized by a mild humid climate that is primarily controlled by variation in NE Pacific atmospheric circulation patterns of the Aleutian Low (AL) and North Pacific High (NPH), as well as the jet stream, and the equatorial El Niño/La Niña cycle (ENSO). Less well-understood, regionally modified, decadal and centennial scale cycles (e.g., the Pacific Decadal Oscillation (PDO)) are superimposed on these weather

* Corresponding author.
*E-mail address:* tpatters@ccs.carleton.ca (R.T. Patterson).

0025-3227/$ - see front matter © 2007 Elsevier B.V. All rights reserved.
doi:10.1016/j.margeo.2007.04.003

phenomena (e.g., Minobe, 1999; Ware and Thomson, 2000).

Anoxic conditions in several coastal British Columbia fjords provide ideal conditions for the preservation of annually deposited laminated sediments, which have provided continuous archives of seasonal climate changes since deglaciation in southern parts of the British Columbia coast (e.g., Nederbragt and Thurow, 2001; Chang et al., 2003; Patterson et al., 2004a,b, 2005). However, much less is known about the climate records preserved in anoxic basins in fjords found in more northerly areas. This study was carried out on a partially laminated sediment core (VEC02A07) obtained from Alison Sound within the Seymour–Belize Inlet Complex (SBIC) on the central BC mainland coast (Fig. 1A). We employed time-series analysis of particle size measurements sampled through the core as well as on line-scans derived from X-ray images of sediment slabs (showing variability in both laminae colour and thickness) to reconstruct a high-resolution record of diatom productivity, precipitation and climate change through the late Holocene. Box-counting, low-pass filtering, wavelet (WA) and spectral analysis (SA) are statistical techniques that were used to detect and quantify the observed high-resolution sedimentary and climate change patterns. Similar methodologies have previously been successfully utilized to study the sedimentary and climate history of inlets in the southern coastal region of British Columbia (e.g., Nederbragt and Thurow, 2001; Patterson et al., 2004a, 2005) These sedimentary and climate-change patterns were in turn compared with previous late Holocene sedimentary and climate studies carried out in the North Pacific and North Atlantic regions to distinguish local and more widespread phenomena (e.g.,Ware and Thomson, 2000; Pellatt et al., 2001; Raspopov et al., 2004; Razjigaeva et al., 2004).

## 2. Physical setting

### 2.1. Geography

The SBIC, which includes Alison Sound, forms a 1600 km long network of long and deep steep-sided fjords on the central coast of mainland British Columbia (Fig. 1) between latitudes 50°50.2′N and 51°10.6′N, and longitudes 126°30.2′W and 127°40.5′W. The SBIC extends more than 90 km inland from the Nakwakto Rapids, at the Pacific coast, to the mouth of the Seymour River (Fig. 1). Just seaward of the Nakwakto Rapids the SBIC opens to Queen Charlotte Sound and the Pacific Ocean via Slingby and Schooner Channels.

The main arms of the complex are comprised of the east–west trending Seymour and Belize inlets, which reach inland about 70 and 50 km respectively. Alison Sound is a smaller inlet that extends in a northeasterly direction for 20 km off the northern margin of Belize Inlet. Freshwater input from creeks and rivers at the head of the various inlets in the SBIC together with numerous waterfalls along the inlets, which peak during the snow-melt period that starts in May, plays an important role in circulation in the SBIC (Thomson, 1981). Waump Creek, which enters Alison Sound at its head is the most important stream in that inlet.

### 2.2. Climate

The climate of coastal British Columbia is mild. Temperatures that are usually above the freezing point characterize the wet winters typical of the region. As a result, the ocean never freezes over in the SBIC. Summers in the region are characterized by warm days and cool nights (Hare and Thomas, 1979). Mean annual precipitation in the SBIC region is high, averaging 3120 mm (2009 mm–3943 mm) with an average annual temperature of 9.1 °C (5.4–9.4 °C) (Green and Klinka, 1994).

Weather systems in this region are seasonally dominated by the counter-clockwise circulating winds that accompany the Aleutian Low (AL) in winter and the clockwise circulating winds that occur with the North Pacific High (NPH) in summer. The relative position of these pressure systems is in turn influenced by shifts in the positioning of the jet stream (Ware and Thomson, 2000), which is in turn influenced by sunspot cycles (Hameed and Lee, 2003).

The position and clockwise circulation pattern of the AL is responsible for the frequency and intensity of winter storms that strike the SBIC (Miller et al., 1994; Beamish et al., 1999; Chang and Patterson, 2005). Storms that form in the ocean on the southern fringe of the AL travel north eastward towards southern BC and northern Washington and storms that form in the Gulf of Alaska move south eastward toward the coast (Cayan and Peterson, 1989; Trenbeth and Hurrell, 1994). During the spring and summer, when the NPH moves northward and the AL dissipates, less precipitation and clear skies are the dominant features in the area (Thomson, 1981; Chang and Patterson, 2005). Although the position and strength of the AL is characterized by great interannual variability, there have been periods, some of which display cyclicity, when a strong westward position of the AL dominated at longer time-scales (Spooner et al., 2002; Hu et al., 2003; Chang and Patterson, 2005).

### 2.3. Oceanography

The SBIC is adjacent to the oceanographic Coastal Transition Domain (CTD), an area that extends from northern Vancouver Island to Dixon Entrance (Ware and Thomson, 2000). As the name suggests, the CTD is characterized by conditions that are transitional from upwelling conditions to the south in the Coastal Upwelling Domain (CUD) and down welling conditions that prevail in the Gulf of Alaska to the north (CDD). Since the SBIC opens to Queen Charlotte Sound instead of the open ocean, the influence of oceanic upwelling within the SBIC is virtually nil as compared to more exposed inlets like Effingham Inlet on the west coast of Vancouver Island (e.g., Patterson et al., 2004a). However, the SBIC does receive inflow from the open ocean as a result of a phenomena that occurs when a deep current encounters an underwater ridge, such as the sills at the entrance to the SIBC and contained sounds and inlets, which deflects the current towards the surface (Thomson, 1981).

An important characteristic of the bathymetrically steep sides fjords of the SBIC is the presence of sills at the mouths of most of them, which were formed by crushed rock and silt that were deposited as moraines by advancing glaciers. The sills restrict the input of oxygen-rich ocean water into the inlets, which together with a low-salinity wedge caused by riverine input at the surface, results in reduced mixing between surface and bottom waters, forming a stratified water column (Pickard and Stanton, 1980; Thomson, 1981). Restricted circulation in fjord systems such as the SBIC enhances the trapping of organic and inorganic material borne by runoff, making these environments effective nutrient traps. Such environments are ideal for paleoenvironmental research as disturbance at the sediment water interface is minimized due to the high residence time and slow circulation of the bottom waters.

The main sill at the mouth of the SBIC, the Nakwakto Rapids, is only 34 m deep and 300 m wide, and forms a major bottleneck during tidal cycles (Department of Energy, 1979) (Fig. 1). The ebb tide current flow through Nakwakto Rapids reaches velocities of up to 8 m/s, making it one of the strongest tidal currents in the world (Thomson, 1981). The narrow and shallow Nakwakto Rapids forms such an impediment to water flow that it is impossible for sea level with the SBIC to equalize with that of Queen Charlotte Sound during

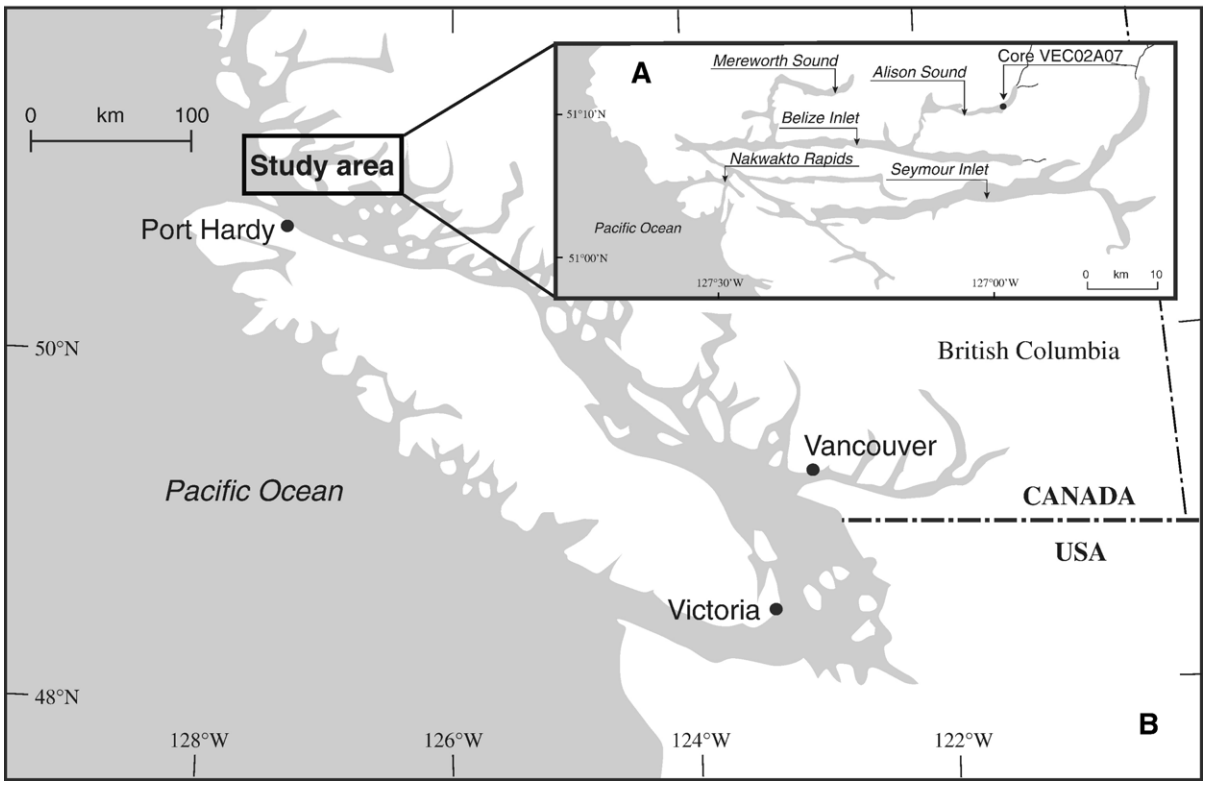


Fig. 1. A: Map of Seymour–Belize Inlet Complex and Smith inlet, black circle: location of Alison Sound core VEC02A07; B: west coast of British Columbia, Canada.

ebb tidal flow, resulting in a tidal range of more than 2 m in Queen Charlotte Sound and a maximum of only 1.3 m in the interior of the SBIC (Fisheries and Oceans Canada, 2003).

### 2.4. Alison Sound

Water depth in the deepest part of Alison Sound is 135 m but two sills at the mouth of Alison Sound significantly restrict circulation into this inlet (Fig. 1). The outermost one, located at the juncture of Alison Sound with Belize Inlet, is 31 m deep while the second, just inside the mouth of Alison Sound, is 30 m deep.

Vertical salinity profiles measured throughout the basin during an August 2000 research cruise of the CCGS Vector (R. Thomson, personal communication, 2003) revealed well-developed estuarine-type stratification, typical of similar silled fjords observed elsewhere (Thomson, 1981). In environments where estuarine circulation patterns prevail, higher salinities at the bottom of a basin than at the surface leads to stagnant water at depth, which eventually results in development of dysoxia or anoxia (Thomson, 1981). In the case of Alison Sound salinity in the sound varies from 10–15‰ at the surface to 28‰ at the bottom. The bottom waters of Alison Sound are anoxic as well (0.00–0.06 ml oxygen/l water).

## 3. Material and methods

The 872.4 cm long Alison Sound piston core (VEC02A07; 51°10.5′N, 127°56.1′W) was collected in 132 m water depth where anoxic bottom water conditions presently prevail. The core site was selected as it was from near the deepest part of the inlet (maximum depth 134 m) in a flat area near the center of the sound where the influence of slumping would be minimized.

### 3.1. X-ray image processing

A set of 46 continuous sediment slabs, up to 20 cm long, 3 cm wide, and 1 cm thick were cut from the full length of the core and X-rayed to facilitate interpretation of contained sedimentary structures. Image analysis of core intervals containing laminated sediments were used to simultaneously measure two characteristics: (1) X-ray grey-scale values and (2) lamina thickness values (Prokoph and Patterson, 2004).

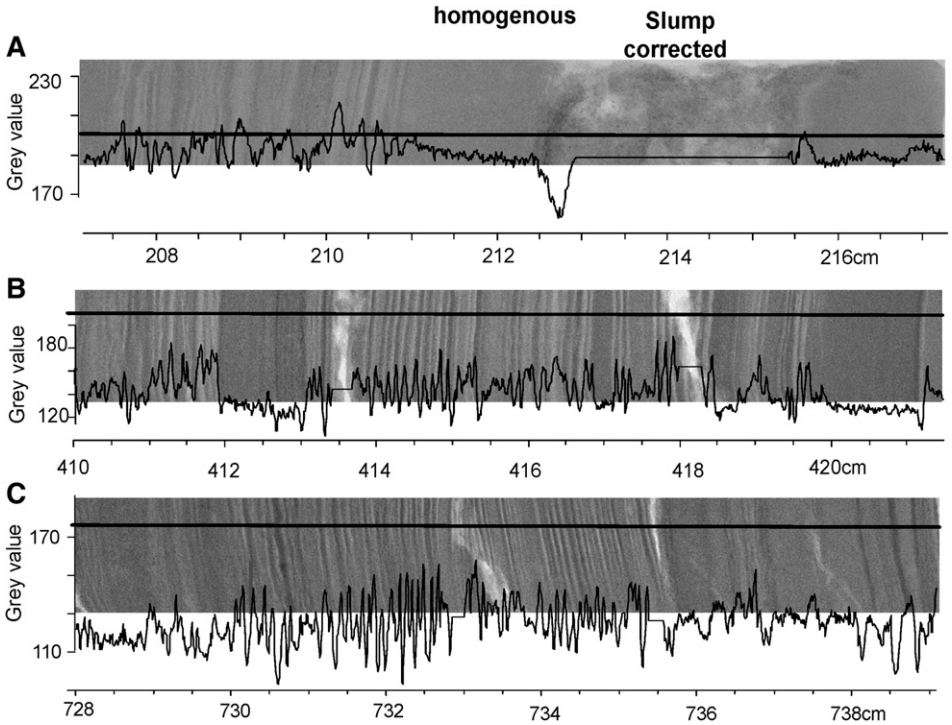


Fig. 2. X-ray scan images of three 3 cm wide and ~1 cm thick sediment slabs of Alison Sound core VEC02A07; grey bar: 10-pixel wide line-scan location; on bottom of each scan: calibrated grey value data (110 = light grey, 230 = dark grey-black). Note that cracks, slumps, and other disruptions in the core are corrected by linear interpolation.

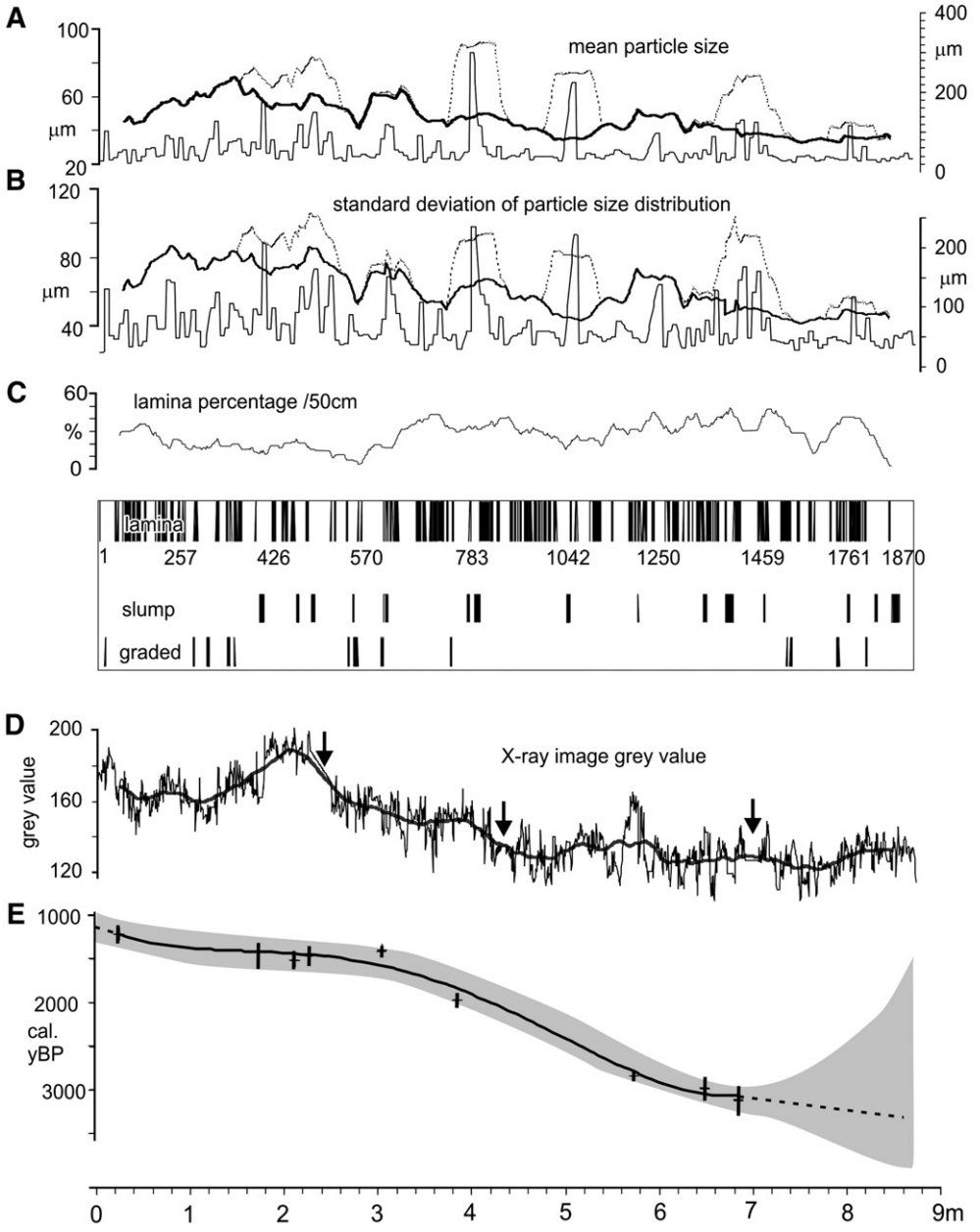


Fig. 3. Sedimentary data and age model of the Alison Sound core VEC02A07. A: Solid line: mean particle sizes of 155 samples; dotted line 50/5 cm moving average of mean particle size; bold line: 50/5-cm moving average of mean particle size after removal of data from slumps; scale on right: raw data, scale on left: smoothed data. B: Solid line: standard deviation (1 s) of particle size distribution of 155 samples; dotted line 50/5 cm moving average of 1 s of particle size distribution; bold line: 50/5-cm moving average of 1 s of particle sizes distribution after removal of data from slumps; scale on right: raw data, scale on left: smoothed data. C: Top: lamina percentage per 50 cm sliding window of total sediment, below: location of all lamina with total lamina count at 1 m intervals, slumps and graded sediment in core; remaining empty space marks homogenous (massive) intervals. Note that lamina concentration appears over represented due to the thickness of the lines. D: X-ray image grey value time series (solid line) and 50/0.25 cm moving average (bold line). Arrows mark intervals with >4 cm of lost core. E: Age–depth model: solid line: 4th degree polynomials; grey shaded area: 95% confidence interval of 4th degree polynomials; crosses: location of $^{14}C$ calibrated ages with ±95% confidence intervals.

From the digitized X-ray images we extracted sediment colour data at a 256 grey-scale resolution (0=black, 255=white) from 10 pixel (~1 mm) wide line scans run perpendicular to stratification, using the software IMAGEJ (Rasband, 1997, and later updates). The line scans were calibrated using trend lines to correct for any

variations in image background colour caused by factors such as fluctuation in X-ray intensity, to equal a standard value (e.g., Nederbragt and Thurow, 2001). About 5% of the sediment column was either not recovered during coring, or was disturbed. The disturbed and missing core intervals were carefully delineated and replaced by linearly interpolated grey-scale values (see Prokoph and Patterson, 2004) (Fig. 2). Further editing of the line scans involved the replacement of extreme or artificial grey-scale values (e.g., those caused by small cracks in the core, Fig. 2A) by using adjacent grey-scale values (after Schaaf and Thurow, 1994). The resulting complete time series of X-ray image grey-scale value from the core (Fig. 3D) was 872.3836 cm long (95,527 pixels).

### 3.2. Particle size analysis

One hundred and fifty five sediment samples of about 1 cm thickness were collected for particle size analysis (PSA) at 5 cm intervals through the core (Fig. 3A, B). For PSA, 5 cc of sediment from each sample was placed in a 50 ml centrifuge tube and chemically digested with 25 ml of a 10% hydrochloric acid solution. Hydrogen peroxide was then added to each sample to remove the organic matter from the sediment and again centrifuged down. The particle distribution of each sample was measured using a Beckman-Coulter LS 230plus laser particle size analyzer. Before carrying out particle size analysis a 1% Calgon solution was added to each sample to disaggregate the particles and the default Fraunhofer optical model was applied (Murray, 2002; Van Hengstum et al., 2007).

### 3.3. Age model

Radiocarbon AMS dates from nine wood fragment samples were obtained from the IsoTrace Radiocarbon Laboratory at the University of Toronto and calibrated with standard data set INTCAL98 (Stuiver et al., 1998) (Table 1). We applied a polynomial age–depth model. Other age model types such as spline function have been proven more accurate (e.g., Telford et al., 2004) but could not be applied here because of some reversals in radiocarbon and calibrated ages (Table 1). In addition, the common occurrence of turbidite layers and the incomplete preservation of some lamina prevented us from using lamina counts for model refinement.

### 3.4. Sedimentary proxies used for paleoenvironmental reconstruction

Changes in the type and pattern of marine anoxic sediments can be correlated to changes in the surrounding environment during and after deposition. We extracted and measured proxies from the sedimentary record of the core following methodologies developed by others who previously studied mixed siliciclastic/biotic sedimentary records from anoxic fjord environments elsewhere in coastal British Columbia (e.g., Nederbragt and Thurow, 2001; Patterson et al., 2004a,b; Prokoph and Patterson, 2004). As has been observed elsewhere in the region where laminated sediments deposited under anoxic conditions are found, the lighter-coloured yellowish-green laminae couplet are comprised of diatomaceous-rich sediments typical of spring–summer deposition along the NE Pacific coast, while the darker layers are primarily comprised of clays rich in organic matter and are typical of autumn–winter deposition (Fig. 2). Analysis of grey-scale values derived from scans of core X-rays served as a proxy for mineral and biotic content while simultaneous measurement of lamina thickness values served as a proxy for precipitation and/or productivity (Figs. 2 and 3). As previously observed and as described below analysis of these measurements demonstrate that

Table 1
Calibrated radiocarbon ages of core VEC02 (Alison Sound)

| Sample ID | Description | Depth (cm) | Radio carbon in yr BP | Sediment type | Cal age yr BP | Lamina # | Cal age 95.5% conf. |
|---|---|---|---|---|---|---|---|
| VEC02A07-1-27 | Wood stick | 27 | 1210 | Massive | 1210 | 30 | 685 cal AD–900 cal AD |
| VEC02A07-2-79 | Wood frag. | 176 | 1490 | Slump | 1410 | 377 | 380 cal AD–690 cal AD |
| VEC02A07-2-118 | Wood frag. | 215 | 1580 | Slump | 1522 | 485 | 385 cal AD–600 cal AD |
| VEC02A07-2-134 | Wood frag. | 231 | 1510 | Slump | 1451 | 501 | 420 cal AD–655 cal AD |
| VEC02A07-3-59 | Wood frag. | 308 | 1460 | Laminated | 1392 | 570 | 525 cal AD–655 cal AD |
| VEC02A07-3-140 | Wood frag. | 389 | 1960 | Massive | 1962 | 755 | 60 cal BC–135 cal AD |
| VEC02A07-4/5-18 | Wood frag. | 578 | 2640 | Laminated | 2800 | 1210 | 900 cal BC–760 cal BC |
| VEC02A07-5-72 | Wood frag. | 654 | 2830 | Massive | 2975 | 1440 | 1130 cal BC–825 cal BC |
| VEC02A07-5-108* | Wood frag. | 690 | 2910 | Massive | 3110 | 1490 | 1265 cal BC–915 cal BC (7.8%) |
| | | 690 | | Massive | | | 1265 cal BC–965 cal BC (10%) |
| | | 690 | | Massive | | | 1265 cal BC–965 cal BC (82.2%) |

*Multimodal calibration solution.

the derived mineral content values and precipitation/productivity signals could co-vary independently (e.g., Nederbragt and Thurow, 2001).

### 3.5. Time-series analysis

We used time-series analysis methods that are suitable for both continuous and discrete (e.g., punctuated by events) records due to the complex nature of sedimentation observed in the core (primarily laminated sedients punctuated by sporadic turbidites).

Continuous wavelet analysis (WA) and spectral analysis (SA) were applied on core intervals where continuous sedimentation prevailed. The combination of WA and SA permitted the detection of cycle wavelengths (periodicity), variance, confidence intervals and duration of sedimentary and climate cycles. For wavelet analysis, we utilized the Morlet wavelet as the analysis function (Morlet et al., 1982), which is simply a sinusoid with a wavelength/period modulated by a Gaussian function. An analysis window size of $l=10$ was chosen because it has proven efficient in analyses of climate-related records (e.g., Ware and Thomson, 2000; Gedalof and Smith, 2001). We evaluated the significance of the wavelet coefficients according to the null-hypothesis of random and Brownian-walk noise (e.g., 'white' or autoregressive 'red' noise) (cf., Mann and Lees, 1996; Torrence and Compo, 1998).

For spectral analysis we calculated the power spectra using a 3-frequency lag Hanning–Tuckey window (e.g., Davis, 2002) and calculated the average power spectra from two to four different depth or time intervals, which permit the evaluation of significance intervals for each frequency (e.g., Ware and Thomson, 2000). Confidence levels were quantified by combining the ±2-s confidence intervals of white and red noise after Mann and Lees (1996).

For discontinuous sedimentary pattern analysis we utilized the box-counting analysis (BCA; e.g., Feder, 1988; Prokoph, 1999) methodology that has previously been successfully utilized to distinguish self-organized and random patterns in turbidite sedimentation (e.g., Rothman et al., 1994). BCA is applicable on binary data, in this case presence of lamina versus absence of lamina. We calculated probability $p$ to find an event $p(L)$ at box length $L$ using a modified variant (Prokoph, 1999) of the original BCA definition (e.g., Feder, 1988). In petroleum exploration this BCA method is used to discriminate the 'success ratio' from the probability $p$ to find an event (e.g., Cheng et al., 2000).

We calculated $p(L)$ by $N(L)/N_{max}(L)$ with $N(L)$ representing the total number of events (number of boxes that contain any lamina) and $N_{max}(L)$ as the total number of boxes of size $L$. The counts of $N(L)/N_{max}(L)$ as well as the selection of 40 box sizes $L$ per run were performed using the software TIMEFRAC.C (Prokoph, 1999). The power law relationship between $p(L)$ and $L$ is defined by

$$p(L) = aL^B \quad (1)$$

where $B$ is the scaling exponent, or fractal dimension, and $a$ is a constant. In this application, $a$ represents the probability to find a lamina couplet in a 1-cm sediment interval, and $B$ is dependent on slope geometry, mineralogy, water content, shape and size of the re-deposited sediment. The confidence intervals for $a$ and $B$ were calculated from the slope of the power-law function over several box sizes, and over different 1-m long core intervals.

## 4. Results

### 4.1. Age model

The 4th polynomial age-model derived from nine calibrated $^{14}C$ dates indicates that the sedimentation in the core spanned the interval from ~3500 to ~1000 yr BP (Fig. 3E). The piston corer over penetrated by ~1.2 m when this core was collected resulting in the loss of the last several hundred years of sedimentation. The average sedimentation rate for the entire core was calculated to be ~0.3 cm/yr, but was relatively higher between ~1 and 3.5 m (<0.8 cm/yr) and below 6.5 m (~0.48 cm/yr) (Fig. 3E). Several hundred years of sedimentary record (~1.2 m) were missing from the top of the core, as a result of piston core over-penetration. Since turbidite deposition is virtually instantaneous, the age-model is only valid for depth intervals of >20 cm, which is the maximum interval between laminated sequences (Fig. 3C).

### 4.2. Sedimentology

In general, sediments in the Alison Sound core consisted predominantly of greyish-brown to yellowish-green weakly consolidated clay and silt. The major mineral components were clay minerals and quartz. Major biogenic components were particulate organic matter and diatoms, resulting in darker and lighter colouration, respectively. Four unevenly distributed sedimentary facies were recognized by visual inspection of the core and X-ray images (Fig. 3C). These facies encompassed; (1) annually deposited couplets of light and dark laminae (23%); (2) heterogeneous slumps deposited by debris flows (5%), (3) graded clay–silt layers (2%); and (4) homogenous massive fine-grained sediments without any internal structure (70%). There was no

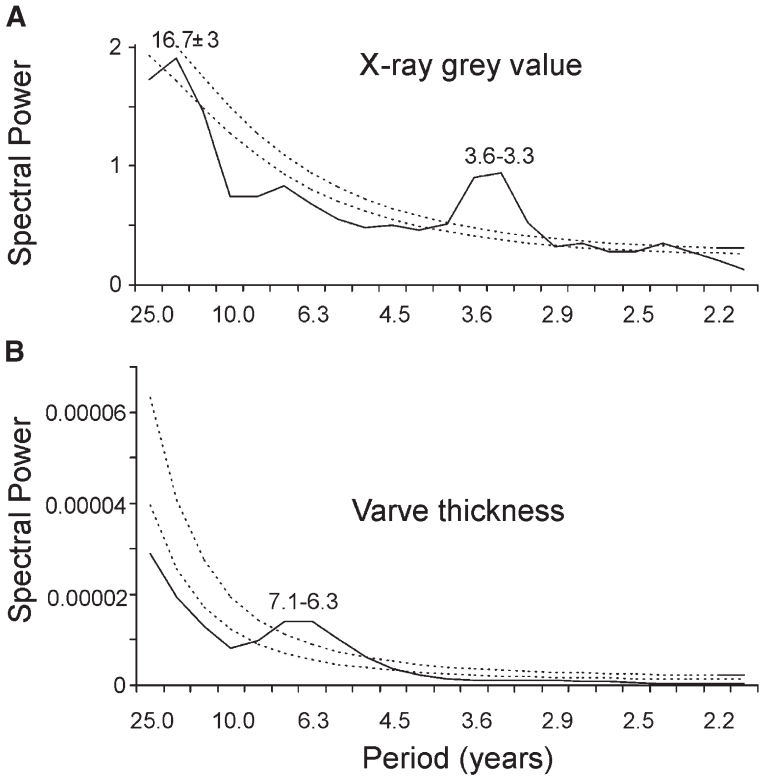


Fig. 4. Spectral power of laminated sequences of the Alison Sound core using a 3-frequency Hanning–Tuckey window; average of stacks of two spectra from two laminated intervals (410–422 cm; 728–740 cm) each, calculated after Davis, 2002; A: X-ray image grey value time series; B: varve thickness (1 dark+1 bright lamina) time series; red noise level (lower dashed lines) and 95% confidence level (upper dashed lines) calculated after Mann and Lees (1996).

evidence of tectonically-derived deposits in the core such as large slumps (>20 cm), or major unconformities.

A total of 1870 lamina couplets were counted, which ranged in thickness from 0.7 to 3 mm (Figs. 2 and 3C). The X-ray derived colour variability between the darker and lighter layers of these seasonally deposited couplets ranged from ~10 to 30 grey-scale units within a 256 unit increment grey-scale, which is significantly above the background noise of five grey-scale units (Fig. 2).

On average, laminae couplets were slightly thicker (~2.1 mm; standard deviation (s.d.)=1.2 mm) in the uppermost two meters of the core than in the lower part (~1.6 mm; s.d.=1.2 mm) (Fig. 2), which could be due to either higher diatom productivity, or wetter conditions, during deposition of the topmost sediments, or the result of less compaction. Laminae concentration is below 100 laminae/m between ~0.8 and 3 m depth, and again below 8.2 m depth (Fig. 3C).

The composition of the massive intervals and slumps are variable with significant quantities (>20%) of angular quartz, wood fragments, and occasionally carbonate debris. Despite this sedimentological variability, there is no evidence of bioturbation, macrobenthos, or other indications of seafloor oxygenation throughout the core. Slump deposits are generally a slightly more yellowish-greyish colour due to more sand-sized quartz content than the other sediment types (Fig. 2A). We therefore conclude that these generally coarser slumps are derived from a slightly different source than the other sediments in the core. As the slumps were deposited under a higher energy regime they may reflect an increased terrigenous input. The margins of Alison Sound both above and below the waterline are steep and there is evidence on the mountainous slopes adjacent to the inlet of periodic land slides that would episodically provide large quantities of terrigenous sediment to the basin.

The distribution of mean particle size and the particle size standard deviation throughout the core show similar trends (Fig. 3A, B). The mean particle size varies between 30 μm and 300 μm, with all samples having a mean particle size of >100 μm showing evidence of being at least partially derived from a slump deposit (Fig. 3A). The standard deviation of the particle size distribution shows

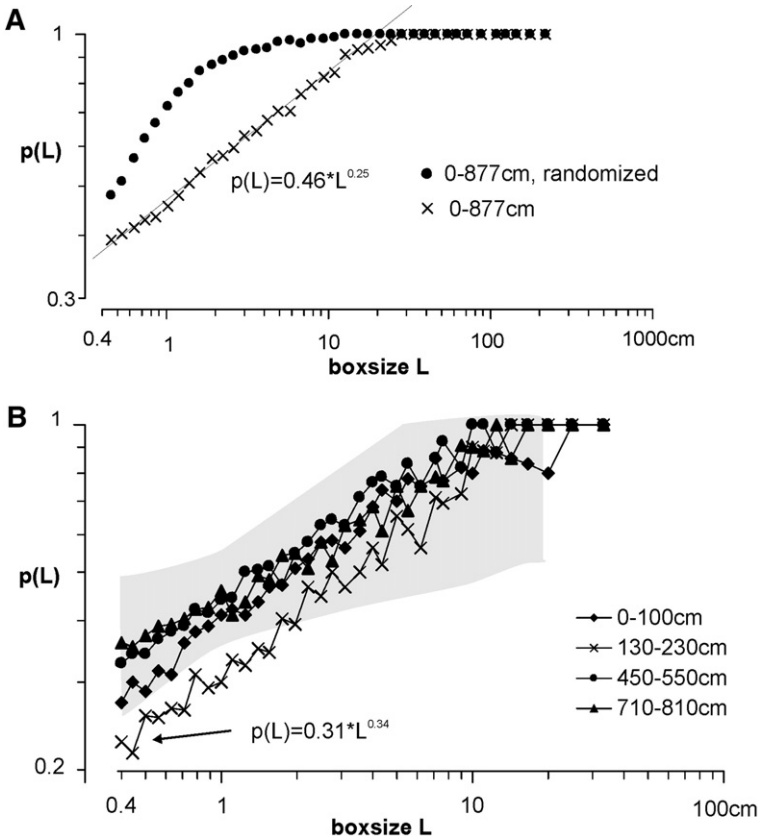


Fig. 5. Log–log plot of probability ($p$) of finding a lamina couplet in interval (box) of length $L$ in the Alison Sound core VEC02A07. A: Entire core for observed and randomized data; B: four 1-m long core segments with no missing core (100% recovery); grey area: 95% confidence interval for log–log model $p(L)=0.46\pm0.1*L^{0.25\pm0.12}$ for the entire sedimentation interval; note that the interval from 130 to 230 cm has a similar parameter $b$ as the other segments but a significantly lower parameter $a=0.31$ (=probability of finding a lamina in a 1-cm long interval).

the same pattern, with much higher values being measured in the inferred slump deposits (>100 μm). Both particle size and X-ray grey-scale values increased from the bottom of the core up to ~2 m depth and decreased again above this level toward the top of the core (Fig. 3A, B, D).

### 4.3. Sedimentation pattern analysis

The general sedimentation pattern observed within the core is characterized by a laminated background sedimentation that is frequently interrupted by turbidites and bottom current related re-deposition that formed massive intervals. Sedimentation on core interval-scales of >0.4 cm is predominantly discontinuous, because of the occurrence of turbidites.

The longest continuous depositional intervals occur as sequences of consecutive lamina couplets between 411 and 419.5 cm and from 728 to 735.5 cm depth, which respectively represent continuous 78 and 70 year depositional records (Fig. 2B, C). Spectral analysis indicates that a periodic pattern at >95% confidence exists for repetition of 3.3–3.6 years in grey-scale variability, and ~6.5 years in lamination thickness variability (Fig. 4). In addition, a 16.7±3 year periodicity at >90% confidence may be assigned to the X-ray grey-scale values.

Box counting analysis reveals that the pattern of laminated versus turbidite sedimentation approaches a straight line in a log–log plot (i.e., power-law) at length scales from 0.4 cm to ~13 cm and at different depth intervals of the core (Fig. 5). This pattern cannot be produced by a purely random occurrence of laminae couplets (Fig. 5A). The probability of lamina occurrence $p(L)$ departs from the straight line at ~13 cm and become completely horizontal ($p=1$) at 25 cm interval length (Fig. 5A). Between 0.4 and 13 cm length-scale the best fit (±2 s error) for the probability of finding evidence of laminated sedimentation follows a power law model

$$p(L) = 0.46\pm0.1*L^{0.25\pm0.12}$$

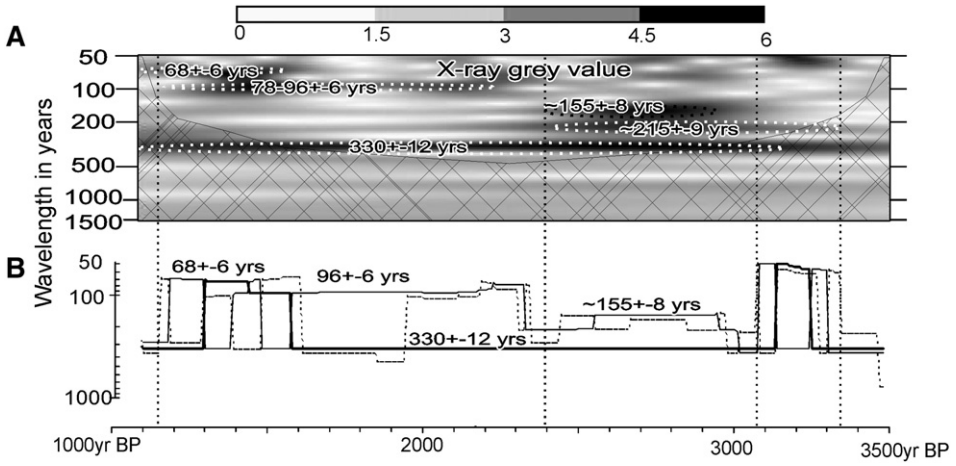


Fig. 6. Wavelet analysis (using Morlet wavelet with 10 cycle window) of X-ray grey value of entire Alison Sound core (VEC02A07) in time-scale (5-year spacing). A: Wavelet scalogram with wavelet coefficient expressed in signal amplitudes as shades of grey (see amplitude scale on right). Gridded area marks wavelength-location space in which the amplitude of long wavelengths is up to 50% suppressed and dotted lines mark 95% significance versus white noise (Torrence and Compo, 1998). B: Temporal evolution of three most intense periodic signal bands. Vertical dotted lines mark distinct changes in the major cycle pattern at ~1130±120 yr BP, 2380±400 yr BP, 3080±150 yr BP, 3370±150 yr BP.

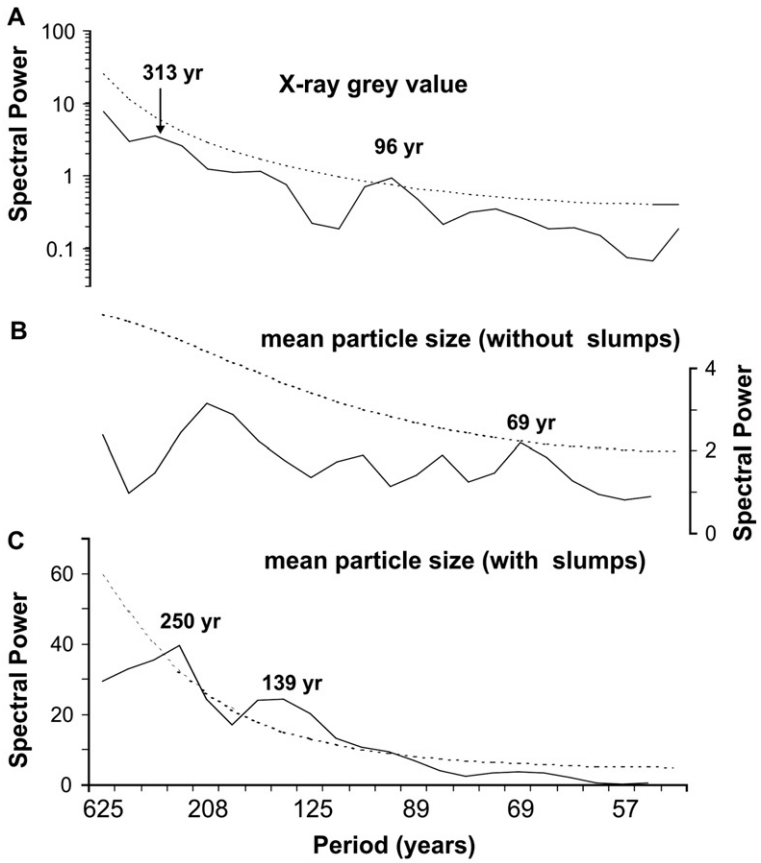


Fig. 7. Spectral power (3-frequency Hanning–Tuckey window, average of two spectra of two 1250-yr sequences each at 25 year sample-intervals); A: X-ray image grey value time series; B: mean particle size with replacement of slumps by interpolated data (135 raw data) time series; C: mean particle size time series from 155 raw data; dashed line mark 95% confidence level for red noise (after Mann and Lees, 1996).

Thus, the sedimentary processes on the 0.4 to ~13 cm length-scale range is scale-invariant with a box-counting (i.e., fractal) dimension of $B=0.25$, expect for the core interval from 130 to 230 cm with $B \sim 0.34$ (Fig. 5B). For example, over a depth interval $L=1$ cm the parameter $a=0.46\pm0.1$ indicates that, in average,

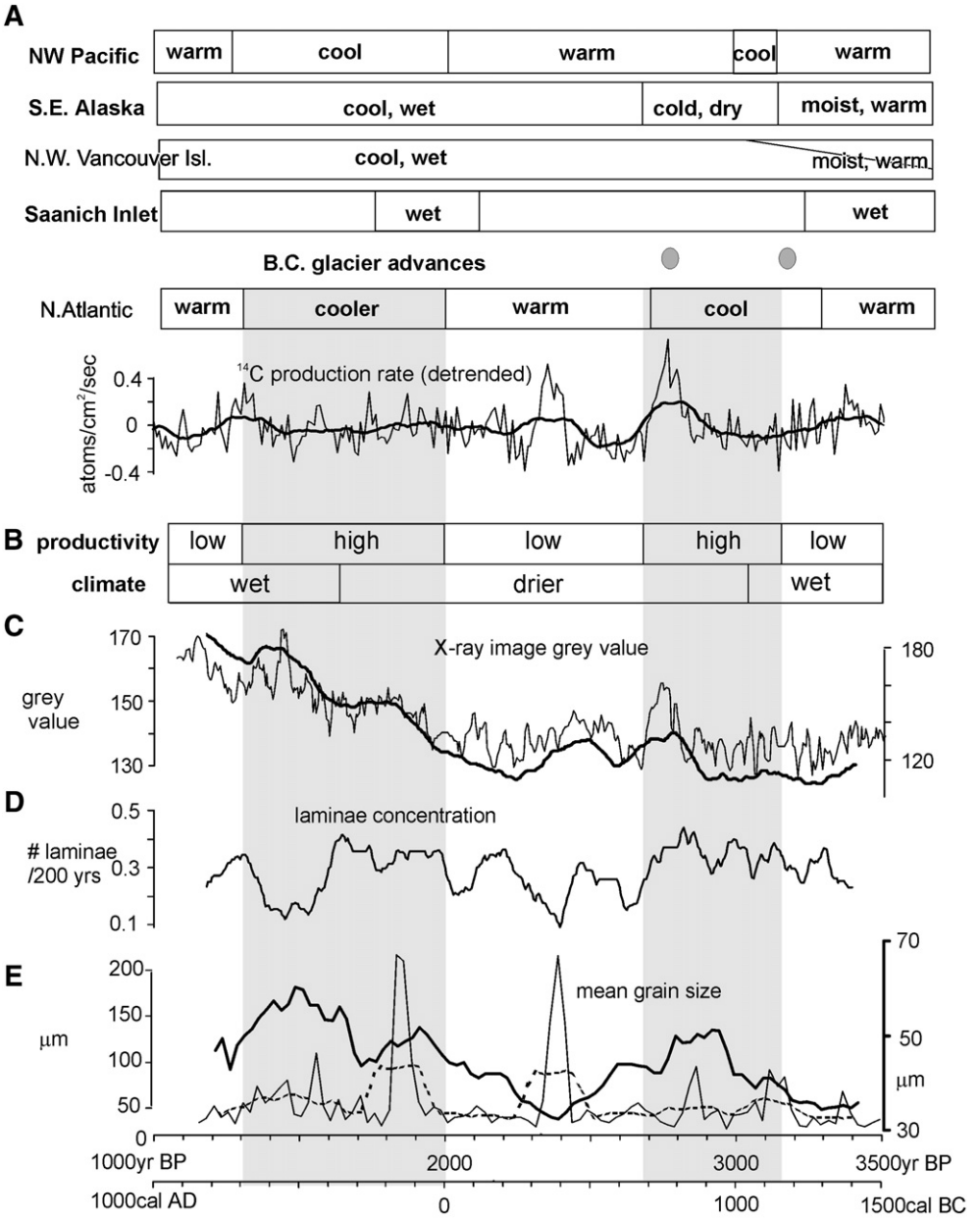


Fig. 8. Comparison of regional and global climate scenarios with data from Alison Sound, B.C. A: Regional and global climate signals from top to bottom: NW Pacific (Razjigaeva et al., 2004), climate intervals in Alaska Northern Vancouver Island from vegetation pattern (Hebda, 1995; Pellatt and Mathewes, 1997; Pellatt et al., 2001). Lamination pattern at Saanich Inlet (Southern Vancouver Island); grey dots mark major onsets of two glacial advances in B.C., grey dots mark major onsets (after Pellatt and Mathewes, 1997), cool and warm intervals from the North Atlantic after Bond et al. (2001). Note that the duration of the changes is up to 500 years. Detrended radio nuclide $^{14}C$ production rate (solid line: 10 year sample interval, bold line 200 year moving average) with a $2\sigma$ age-uncertainty of is up to ±100 years (Bond et al., 2001). B: Suggested general pattern of productivity and precipitation at Alison Sound, B.C., this study; C: X-ray image grey value of the Alison Sound core (VEC02A07) in time-scale, solid line: 5 year data interval (scale on the left), bold line: 200 year moving average (scale on the right); D: lamina concentration (/100%) per 200 years; E: mean particle size in time-scale: solid line; 25 year spaced data; dashed line: 200 year moving average (scale on left), bold line: mean particle size without slumps, 200 year moving average (scale on right).

with $p(L) \sim 46\%$ probability at least one lamina couplet can be found. The parameter $a = 0.31$ suggests that large turbidite flows are particularly frequent through the 130–230 cm interval of the core (Fig. 5B), probably as the result of increased background sedimentation and increased slope instability perhaps related to increased precipitation. The approach of saturation ($p > 0.95$) at ~13 cm depth scale indicates that more continuous sedimentary processes, apart from self-organization, operate at longer length and time-scales.

For WA and SA we transformed the sedimentary record into a time-scale to allow for correlation with potential external forcing factors and similar sedimentary sequences elsewhere. We consider the age-model (Fig. 2E) and the results from box-counting analysis robust enough to evaluate variability on length-scales of >13 cm (i.e., time-scales of >50 years).

Wavelet analysis of grey-values shows a narrow-band 330±12 year periodicity throughout the complete ~2500 year record (Fig. 6A, B). Periodicity in the 68–96 year wavelength occurs from ~1130 yr BP to ~2350 yr BP. Periodic cycles of ~155–215 years appear from ~2350 to ~3350 yr BP. The amplitude of all of these cycles is at >5 grey-scales, and thus significantly above the white noise level (see Fig. 2). We also tested the data against a Brownian walk model (cf. Turcotte and Newman, 1996). This showed that persistent periodicity in the 330 year band at a grey-scale amplitude value of >5 cannot be reproduced by a random long-term memory process.

Spectral analysis of stacked power spectra from two 1250 year long intervals in the CORE show that a 96 year cycle observed in X-ray grey-scale values is >95% significant (Fig. 7A) assuming a combined red noise+white noise model (Mann and Lees, 1996). The reduced 90% level of confidence associated with the 313-year cycle may be due to the use of a wider smoothed frequency band for SA than was used for the WA.

Periodicities of >95% confidence exist at 250-year and 139-year cycles for the particle size data including values obtained from intervals of slumps (Fig. 7C). The mean particle size time series becomes very noisy when slump deposits are removed (Fig. 7B). Consequently, the sediment volume that is moved by slump deposits probably belongs to the primary, originally laminated deposition from inside the sedimentary basin.

Grey-scale values, lamina concentration, and particle size data form two superimposed millennial-scale cycles (Fig. 8C–E). This two-cycle trend is particularly well pronounced in the particle size data following removal of the slumps (Fig. 8E), and is overprinted by an upward increasing trend in the X-ray grey-values (Fig. 8C).

## 5. Discussion

### 5.1. Nature of non-linear sedimentary patterns in Alison Sound

The late Holocene sedimentation patterns identified in the sedimentary record of Alison sound are characterized by intervals of periodic cyclicity, scale invariance, and several different long-term depositional trends at a variety of core length scales varying from 0.1 to 7 m over a period of ~2500 years. In addition, there is a significant amount of noise in the sedimentary signals that are either the result of unknown short-term events, non-periodic and non-persistent environmental changes in the sediment basin, or time-scale errors due to distortions in the age–depth model.

Our results suggest that sedimentary processes active on <13 cm core length-scale range are scale-invariant and show evidence of self-organized criticality (Bak et al., 1988). Self-organized criticality describes how continuous background processes (e.g., incremental piling of sand or snow) may be interrupted, discontinuously, by abrupt 'destructive' events of varying scale (e.g., avalanches) as a result of the attainment of critical parameters (e.g., exceeding angle of repose). In the case of gravity-flow generated turbidites on the margins of Alison Sound, sediment builds up until gravity overcomes friction resulting in destabilization of the pile. Slumping occurs until the kinetic energy of the process is exhausted and friction is again greater than the momentum of sediment transport, resulting in the resumption of background sedimentation. Scale-invariant turbidite sequences have been reported for deep sea fans (e.g., Rothman et al., 1994), but evidence of self-organized criticality is novel for sedimentation in narrow coastal inlets. At the core location Alison Sound is ~1 km wide and 130 m deep with a sufficiently steep slope to produce self-organized debris flow avalanches (Embleton and Thornes, 1979; Bak et al., 1988). The observed massive, finely grained core intervals are most likely derived from disturbed mud-clouds generated in relatively deep portions of the basin. In contrast, slump deposits are probably the result of coarser grained gravity flows from higher up on the slope of the inlet (Fig. 9).

The probability of finding laminated sediments that were deposited in situ increases at a power gradient of $B = \sim 0.25$. The $B$-value reflects the 'equilibrium' submarine slope gradient required before there is any possibility of a self-organized re-depositional process occurring. In the absence of tectonic activity at the core location, the slope gradient that has in Alison Sound has been primarily dependent on the sediment particle size,

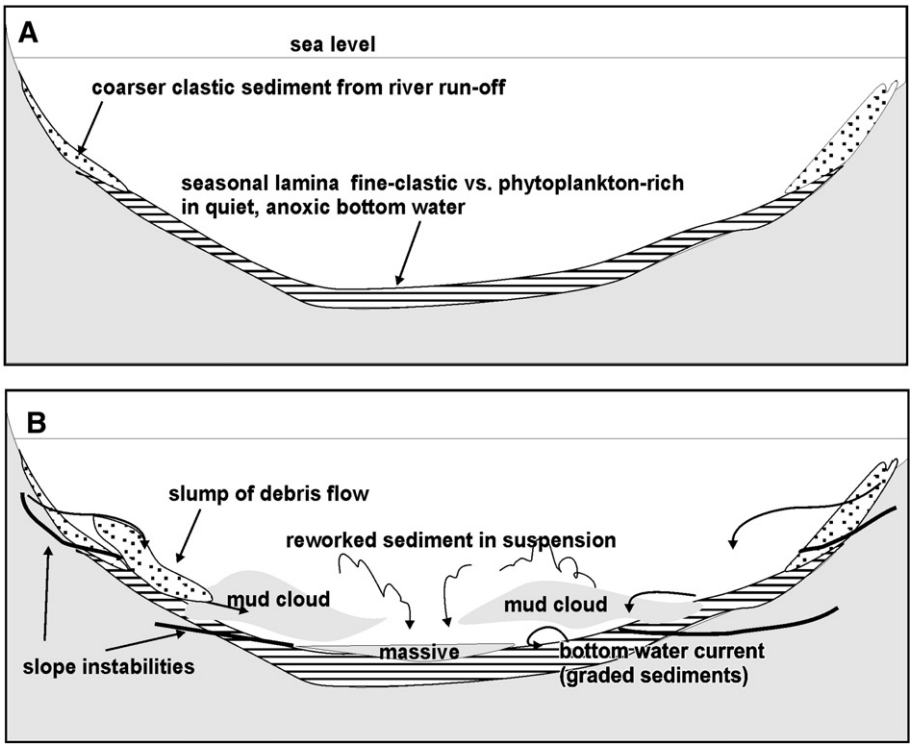


Fig. 9. 2-stage sedimentation model for late Holocene in Alison Sound, B.C. A: "Quiet background'-sedimentation in anoxic bottom by seasonal deposition of diatom-rich (bright) summer and clay-rich (dark) winter lamina. Note that coarser-grained sediments (e.g., psammitic quartz) are trapped at the basin margins. B: Turbidite sedimentation of three sediment types: coarse-grained debris flows from the inlet margin = slumps; disturbed, mixing mud clouds of reworked lamina couplets that deposit as non-sorted homogenous ('massive') fine-grained sediments; bottom currents that lead to graded sediments.

geometry, density, and water content. Two additional factors; (1) changes in sea level; and (2) any increase in river runoff, also influence submarine slope gradient and thus have a direct impact on the probability of annually deposited laminae being preserved. If, for example, sea level rises without significantly increasing the water surface area as would be the case in steep sided Alison Sound, then increasingly larger and more frequent episodic submarine avalanches would have to occur to maintain slope stability. An increase in sediment supply as a result of an increase in river run-off during wet periods would also lead to more re-deposition, and a generally lower probability of laminae preservation. Under both of these scenarios, the percentage of lamina preserved relative to the total depositional package (i.e., *a*-value) decreases, as was observed in the 130–230 cm interval of the core deposited at ~1600–1400 yr BP (Figs. 3 and 9C–E). Thus, the *a*-value fluctuates more than the *B*-value in a self-critical system in order to balance out any external variability (see Fig. 5B).

Based on the scale-range (<13 cm) observed in the turbidite pattern of the ACS core, we conclude that most paleoenvironmental information in the sedimentary record has been destroyed or homogenized at time-scales of less than ~50 years.

### 5.2. Nature of cyclic sedimentation in Alison Sound

In the two surviving core intervals with longer records of laminated sediments (Fig. 2B, C) cycles of ~17±4, ~3.5±0.5 years were observed from the X-ray grey-scale values, and of ~6–7±1 years in couplet thickness.

The observed 6–7 year cycle is very similar to an ~6-year cyclicity that has elsewhere been detected in radiocarbon concentrations from the 1540–1720 AD interval (Raspopov et al., 2004). Raspopov et al. (2004) interpret the cycle as a possible interference pattern derived from longer solar activity cycles. We have no physical explanation for the observed 3–4 couplet cyclicity, which is easy detectable from the grey-scale value variability (Fig. 2C).

The ~17±4 year cycle is of particular interest as it is similar to a ~17-year climate cyclicity that has previously been inferred from analysis of North American tree-ring growth patterns (Raspopov et al., 2004) and drought cycles (Cook et al., 1997), as well as the high-

frequency 15–15 year band portion of the PDO (Ware, 1995; Minobe, 1999; Gedalof and Smith, 2001). This ~17-year peak can be interpreted as either the result of an interference pattern within the ~23 year Hale ($\nu_H$) and ~88 year Gleissberg ($\nu_G$) solar activity cycles, caused by a non-linear positive feedback ($\nu_H+\nu_G$) in the ocean–atmosphere systems (Raspopov et al., 2004), or by a non-linear model of physics within the coupled ocean–atmosphere systems without external control (Latif and Barnet, 1996).

At longer time-scales (>15 cm — i.e. >50 years) a ~68–96 year cyclicity is detectable from analysis of the X-ray image grey-scale values from ~2300 to 1100 yr BP (Figs. 6 and 7A). These cycles, as well as all other longer X-ray derived sediment-colour cycles recognized, are the result of bottom-water-turbulence generated temporal changes in the proportion of silica rich (bright) and clay rich (darker) sediment, which may also result in an averaging of the colour of the laminated segments. In addition to originating as disturbed laminated sediments, non-laminated sediments transported into the anoxic basin center may also contribute to the sedimentary sequence. Similar global quasi-periodic ~80–90 year climate cycles have been attributed to periodic fluctuations in the sunspot number and solar irradiance, known as the Gleissberg Cycle (Gleissberg, 1958). The Gleissberg cycle has been detected in numerous late Holocene paleoclimate proxy records including Arctic ice-cores (Appenzeller et al., 1998), sub-arctic tree-ring width (Raspopov et al., 2004), fish stock fluctuations and X-ray image grey values on SW Vancouver Island (Patterson et al., 2004b).

The alternation bright/dark sedimentary sequences where the Gleissberg cycle predominates in the core occurs independently of coarser grained and quartz-rich slumps (Fig. 7B, C) suggesting that this cyclicity reflects fluctuations in diatom productivity rather than mineralogical change. The strength and position of the AL and NPH in the NE Pacific has been documented to oscillate at Gleissberg Cycle periodicities and to have a significant influence on marine productivity, particularly diatom production, in upwelling influenced areas (Patterson et al., 2004a; Chang and Patterson, 2005). Alison Sound is deep within the SBIC and is not strongly influenced by upwelling at any time. However, the relative influence of the AL and NPH does have a significant influence on precipitation within the SBIC. In a detailed analysis of Holocene diatoms from nearby Frederick Sound, also within the SBIC, Wigston (2006) observed that diatom production there also varied at the same periodicities as Gleissberg cycles. We hypothesize that during periods when the AL was on average stronger and in a more easterly position wet and cloudy conditions lasted longer into the spring and summer in the SBIC, reducing surface salinities (via direct precipitation, runoff, and an enhanced freshet) and light incidence. These conditions would have resulted in a suppressed spring and early summer diatom bloom. When the AL was on average weaker and the NPH stronger, relatively drier and sunnier conditions would have prevailed, which would have been more conducive to a strong spring and early summer diatom bloom.

Our results suggest that AL/NPH influence resulted in cyclic depositional patterns that both corresponded to ~70–96 year Gleissberg cycle solar irradiance fluctuations on upwelling influenced areas of the BC coast (Patterson et al., 2004a; Chang and Patterson, 2005) and on precipitation in more restricted areas such as the SBIC. In the core this cyclicity was particularly pronounced during the ~2300 to 1100 yr BP interval. Although the absence of the Gleissberg cycle in the core before ~2300 yr BP could be due to an absence of this cycle in the solar activity variability through this interval as has been previously documented during the Maunder Minimum of the Little Ice Age (McCracken et al., 2001), this scenario is unlikely as evidence of the Gleissberg cycle has been observed in laminated sediments of this age from Effingham Inlet to the south (Patterson et al., 2004a). It is more likely that the lack of a Gleissberg cycle signal prior to 2300 yr BP in the core was the result of turbidites disrupting sedimentation, overprinting by other ocean-atmospheric processes, or as a result of errors in the time-scale calibration. Studies on similar sedimentation during this time interval are necessary for further clarification.

Cycles of ~139–155±8 years, derived from both sediment X-ray grey-scale values and particle size data, are particularly abundant from ~3100 to 2300 yr BP (Figs. 6 and 7C). Reports of similar non-periodic multi-decadal cycles of ~110–180 years from elsewhere (e.g., Castagnoli et al., 2002; Dean et al., 2002) have been attributed to major fluctuations in solar irradiance, that resulted in several worldwide cool periods through the last millennium. In Alison Sound, this cyclicity is pronounced in the particle-size variability, particularly when coarser slump deposits are included (Figs. 7C and 8E). Again we cannot exclude the possibility that this cycle is a result of interference related to the turbidite deposition scenario.

High amplitude and persistent 250–330±12 year cycles are recognized in all the sedimentary records from the core (Figs. 6 and 7). As this cyclicity is also well pronounced in particle size data where slumps are included (Fig. 7C), we suggest that this cycle is controlled by changes in terrigenous sediment supply and precipitation, and not diatom productivity. It is doubtful

that this cycle is purely random (e.g., Brownian-walk) or that it is the result of interference of this cyclicity with turbidite deposition, because of the persistent and narrow-bandwidth displayed at this cycle frequency (Fig. 6A, B). Cycles of similar duration were also recognized in Effingham Inlet (Patterson et al., 2004a) and on the Great Plains of North America, where they have been associated with intervals of drought (Yu and Ito, 1999; Dean and Schwalb, 2000; Dean et al., 2002).

Long-term trends and two possible millennial-scale cycles were observed in some of the sedimentary proxy records examined (Fig. 8C–E). Similar millennial scale cycles have been recognized in paleoclimate records throughout the northern hemisphere (e.g., Esper et al., 2002; Hu et al., 2003), and have been correlated to fluctuations in solar irradiance (e.g., Bond et al., 2001). In the specific case of this core, millennial-scale cycles can only be recognized if slump-data are excluded (Fig. 8E). We therefore conclude that this cycle reflects fluctuations in marine productivity (see discussion on Gleissberg cyclicity above) rather than being the result of any variability in precipitation patterns. It is also important to note that marine productivity and precipitation are not always coupled and may occur independently. Factors such as slump intensity may in fact be controlled by long-term trends in the tectonic pattern than by the millennial cyclicity.

Our results suggest that the long-term sedimentary pattern in Alison Sound is characterized by millennial-scale marine productivity cycles, and by periods of increased terrigenous sediment supply, high sedimentation rate, as well as slumps before ~3100 yr BP, and after ~1700 yr BP (Figs. 3C, D and 8B). We also conclude that climatic variability at annual, multidecadal and millennial scales impacted marine primary productivity, precipitation, runoff, weathering and temperature, at least periodically. Where laminated sediments are found there is evidence that higher-frequency climatic fluctuations (multiannual to multidecadal) were important throughout. However, these signals cannot be fully resolved in this core due to overprinting caused by episodic turbidite sedimentation.

### 5.3. Regional and global correlations of climate shifts and cycles

Many of the recognized sedimentary cycles and non-cyclic patterns identified in the core can be correlated with known climate and oceanographic changes in the North Pacific region, and partially to celestial climate driver proxies (Fig. 8; Table 2). From previous studies it is known that through much of the Holocene climate

Table 2
Summary of sedimentary cycles observed in Alison Sound

| Cycle length (years) | Persistency | Duration (years) |
|---|---|---|
| *1* | np | 1000 AD–1500 BC |
| *~3.5* | np | 1000 AD–1500 BC |
| *6–7* | np | 1000 AD–1500 BC |
| ~17 (10–22) | np | 1000 AD–1500 BC |
| 68–96 | np | 900–1300 BC |
| 135–160 | p | 100–1500 BC |
| 155–215 | p | 1000 AD–100 BC |
| 250–330 | p | 1000 AD–1500 BC |
| 1000–1500 | p | 1000 AD–1500 BC |

Italic: cycle length from lamina length estimation.
np — non-persistent.
p — persistent.

along the NW coast of British Columbia has been subject to considerable climate variability (e.g., Hebda, 1995; Ware and Thomson, 2000; Chang and Patterson, 2005; Galloway et al., in press). These climatic trends have not been gradual though, occurring in a series of steps with some regional differences and delays.

Climate cycles in the NE Pacific occur at annual to millennial scales. This climate variability has had a major impact in coastal fjords, including the SBIC, by influencing fluctuations in marine bioproductivity as well as the rate of weathering of exposed rocks in the catchment area. For example, warm and wet climate regimes result in higher clastic, clay-rich input, and more submarine slumps due to the higher erosion rate. In contrast, intervals when cooler and dryer climate conditions prevail commonly results in greater marine productivity and a higher rate of sedimentation from diatom frustules raining to the fjord bottom. During these dryer intervals the clay content of sediments being deposited is also reduced due to a decrease in coastal erosion.

A known major climate shift from a cooler, wet climate to even wetter conditions occurred at ~4000–3300 yr BP (e.g. Hebda, 1995, Pellatt and Mathewes, 1997; Pellatt et al., 2001; Patterson et al., 2004a). The high percentage of preserved laminations in the sediments, relative brightness and increased particle size in background sedimentation deposited in the ~3150–2700 yr BP interval (Fig. 9C–E) correspond to the development of neoglacial conditions in the Cascadia region and Alaska (Pellatt et al., 2001), and in the NW Pacific (Razjigaeva et al., 2004). A major climate shift from 4000 yr BP to 3000 yr BP has also been recorded from the Cariaco basin (Haug et al., 2001), Palmer Deep (Domack et al., 2001) and the Santa Barbara Basin (Cannariato et al., 2003). This event is well documented in palynological proxy records from sites around British Columbia, which record widespread and regionally

variable climate change about that time (Pellatt et al., 2001). A climatic shift to wetter climate is also prominent in the laminated marine sediment records from Saanich and Effingham inlets on the southern coast of Vancouver Island (Nederbragt and Thurow, 2001; Patterson et al., 2004a). As was observed in Saanich Inlet, changes in precipitation are not necessarily correlated to warmer/cooler conditions or variability in productivity (Nederbragt and Thurow, 2001).

The most prominent and best dated sedimentary perturbation in the core (see Table 1) occurs at ~2900–2700 yr BP and correlates well with a major cooling period and glacier advance in NW America, NE Russia, and the North Atlantic (Fig. 8). The widespread nature of this event is also indicated by its correlation with an interval of high $^{14}C$ cosmogenic nuclide production. High $^{14}C$ cosmogenic nuclide production indicates an increased cosmic ray flux, which leads to increased cloud cover and consequently cooler global conditions (Bond et al., 2001; Carslaw et al., 2002; Veizer, 2005; Scherer et al., 2007). A similar, but weaker correlation exists from ~2000 to 1300 yr BP between higher primary productivity in the NE Pacific and cooler conditions in both the North Pacific and North Atlantic (Fig. 8). It may have also been wetter during this interval in the North Pacific region.

## 6. Conclusions

Marine anoxic sedimentation in Alison Sound is characterized by an interplay of turbidites and intervals of laminated sediments that archive essential components of an ~3500–1000 yr BP depositional and paleoclimate record. Self-organized episodic turbidite sedimentation dominates the sedimentary pattern at sedimentary thickness scales of up to 13 cm and for time-scales of up to 50 years. Detailed climate records are therefore only reliably preserved for time-scales of >50 years, although intervals of annually deposited laminated background sediments at time-scales of 1 to ~30 years are sporadically preserved through the cores. These intervals of laminated sedimentary deposition are most common in the core from ~3150 to 2700 yr BP and from ~2000 to 1300 yr BP. These annually deposited laminae are characterized by couplets comprised of dark-coloured, mineral-rich layers primarily deposited during the fall and winter, and lighter yellowish-green coloured diatom-rich layers primarily deposited during the spring and summer. Marine primary productivity seems to have increased along this portion of the mainland coast of BC during these intervals, which have been both regionally and globally recognized as relatively cold intervals.

Several sedimentary, often non-periodic cycles with wavelengths of ~17 years, 96–70 years, 155–139 years, and 330–250 years are related to fluctuations in precipitation, terrigenous sediment supply, coastal upwelling and marine productivity. These cycles of considerably different frequency suggest a significant climate influence on sedimentation in Alison Sound, which can be partially related to fluctuations in solar irradiance and the ocean-atmospheric system over the North Pacific.

## Acknowledgements

We are grateful to R. Thomson (Department of Fisheries and Oceans, Sidney, British Columbia) V. Barrie and A. Dallimore (Pacific Geoscience Centre, Sidney, British Columbia) for organizing ship time, as well as considerable logistic and technical support, without which this research would not have been possible. We thank Gill Alexander (Queen's University, Belfast) for cartographic support. This research was supported by a Canadian Foundation for Climate and Atmospheric Sciences research grant and Natural Sciences and Engineering Research Council Discovery Grant to RTP. This paper is a contribution to International Geologic Correlation Programme Project 495; Quaternary Land–Ocean Interactions: Driving Mechanisms and Coastal Responses.

## References

Appenzeller, C., Stocker, T.F., Anklin, M., 1998. North Atlantic oscillation dynamics recorded in Greenland ice cores. Science 282, 446–449.

Bak, P., Tang, C., Wiesenfeld, K., 1988. Self-organized criticality. Phys. Rev., A 38, 364–374.

Beamish, R.J., Noakes, D., McFarlane, G.A., Klyashtorin, L., Ivonov, V.V., Kurashov, V., 1999. The regime concept and natural trends in the production of Pacific salmon. Can. J. Fish. Aquat. Sci. 56, 516–526.

Bond, G., Kromer, B., Beer, J., Muscheler, R., Evans, M.N., Showers, W., Hoffmann, S., Lotti-Bond, R., Hajdas, I., Bonani, G., 2001. Persistent solar influence on North Atlantic climate during the Holocene. Science 294, 2130–2136.

Cannariato, K.G., Kennett, J.P., Kennett, D.J., Revenaugh, J.S., Malmgren, B.A., 2003. Millennial and centennial climate variability of the California Current System during the Holocene recorded in Santa Barbara Basin. EOS, Trans. Am. Geophys. Union 84 (46) (Fall Meeting Supplement, Abstract OS22C-03).

Carslaw, K.S., Harrison, R.G., Kirkby, J., 2002. Cosmic rays, clouds, and climate. Science 298, 1732–1737.

Castagnoli, G.C., Bonino, G., Taricco, C., Bernasconi, S.M., 2002. Solar radiation variability in the last 1400 years recorded in the carbon isotope ratio of a Mediterranean sea core. Adv. Space Res. 29, 1989–1994.

Cayan, D.R., Peterson, D.H., 1989. The influence of the North Pacific atmospheric circulation and streamflow in the west. In: Peterson, D.H. (Ed.), In Aspects of Climate Variability in the Western Americas. Geophysical Monograph, vol. 55. American Geophysical Union, Washington, DC, pp. 375–397.

Chang, A.S., Patterson, R.T., 2005. Climate shift at 4400 years BP: evidence from high-resolution diatom stratigraphy, Effingham Inlet, British Columbia, Canada. Palaeogeogr. Palaeoclimatol. Palaeoecol. 226, 72–92.

Chang, A.S., Patterson, R.T., McNeely, R., 2003. Seasonal sediment and diatom record from late Holocene laminated sediments, Effingham Inlet, British Columbia, Canada. Palaios 18, 477–494.

Cheng, Y.C., Lee, P.J., Lee, T.Y., 2000. Estimating exploration ratio by fractal geometry. Bull. Can. Pet. Geol. 48, 116–122.

Cook, E.R., Meko, D.M., Stockton, C.S., 1997. A new assessment of possible solar and lunar forcing of the bidecadal drought rhythm in the western United States. J. Climate 10, 1343–1356.

Davis, J.C., 2002. Statistics and Data Analysis in Geology, 3rd edition. Wiley, New York. 637 pp.

Dean, W.E., Schwalb, A., 2000. Holocene environmental and climatic change in the Northern Great Plains as recorded in the geochemistry of sediments in Pickerel Lake, South Dakota. Quat. Int. 67, 5–20.

Dean, W., Anderson, R., Bradbury, J.P., Anderson, D., 2002. A 1500-year record of climatic and environmental change in Elk Lake, Minnesota I: Varve thickness and grey-scale density. J. Paleolimnol. 27, 287–299.

Department of Energy, M.a.R., 1979. Cape Caution, British Columbia (92 M/4). Department of Energy, Mines and Resources, Ottawa.

Domack, E., Leventer, A., Dunbar, R., Taylor, F., Brachfeld, S., Sjunneskog, C., and ODP Leg 178 Scientific Party, 2001. Chronology of the Palmer Deep site, Antarctic Peninsula: a Holocene palaeoenvironmental reference for the circum-Antarctic. The Holocene 11, 1–9.

Embleton, C., Thornes, J. (Eds.), 1979. Process in Geomorphology. John Wiley and Sons, New York. 436 pp.

Esper, J., Cook, E.R., Schweingruber, F.H., 2002. Low-frequency signals in long tree-ring chronologies for reconstructing past temperature variability. Science 295, 2250–2253.

Feder, J., 1988. Fractals. Plenum Press, New York. 283 pp.

Fisheries and Oceans Canada, 2003. Tides, Currents and Water levels. Canadian Hydrographic Service. www.tides.gc.ca.

Galloway, J.M., Patterson, R.T., Doherty, C.T., Roe, H.M., in press. Post-glacial vegetation and climate history of two frog Lake, Central Coastal Mainland, British Columbia, J. Paleolimnol. doi:10.1007/s10933-007-9091-4.

Gedalof, Z., Smith, D.J., 2001. Interdecadal climate variability and regime-scale shifts in Pacific North America. Geophys. Res. Lett. 28, 1515–1518.

Gleissberg, W., 1958. The eighty-year sunspot cycle. J. Br. Astron. Assoc. 68, 1148–1152.

Green, R.N., Klinka, K., 1994. A field guide to site identification and interpretation for the Vancouver Forest Region. Land Management Handbook, vol. 28. BC Ministry of Forests, Victoria, BC. 285 pp.

Hameed, S., Lee, J.N., 2003. Displacements of the Aleutian Low and the Hawaiian High pressure systems during the solar cycle. Eos, Trans. Am. Geophys. Union 84 (Fall Meeting Supplemental, Abstract SH11E-03).

Hare, F.K., Thomas, M.K., 1979. Climate Canada, 2nd ed. John Wiley and Sons Canada Limited, Toronto. 230 pp.

Haug, G.H., Hughen, K.A., Sigman, D.M., Peterson, L.C., Roehl, U., 2001. Southward migration of the Intertropical Convergence Zone through the Holocene. Science 293, 1304–1308.

Hebda, R.J., 1995. British Columbia vegetation and climate history with focus on 6 ka BP. Geogr. Phys. Quat. 49, 55–79.

Hu, F.S., Kauffman, D., Yoneji, S., Nelson, D., Shemesh, A., Huang, Y., Tian, J., Bond, G., Clegg, B., Brown, T., 2003. Cyclic variation and solar forcing of Holocene climate in the Alaskan subarctic. Science 301, 1890–1893.

Latif, M., Barnet, T., 1996. Decadal climate variability over the North Pacific and North America: dynamics and predictability. J. Climate 9, 2407–2423.

Mann, M.E., Lees, J.M., 1996. Robust estimation of background noise and signal detection in climatic time series. Clim. Change 33, 409–445.

McCracken, K.G., Dreschhoff, G.A.M., Smart, D.F., Shea, M.A., 2001. The Gleissberg periodicity in large fluence solar proton events. Proceedings of 27th International Cosmic Ray Conference Hamburg, Germany, pp. 3205–3208.

Miller, A.J., Cayan, D.C., Barnett, T.P., Graham, N.E., 1994. The 1976–77 climate shift of the Pacific Ocean. Oceanography 7, 21–26.

Minobe, S., 1999. Resonance in bidecadal and pentadecadal climate oscillations over the North Pacific: role in climatic regime shifts. Geophys. Res. Lett. 26, 855–858.

Morlet, J., Arehs, G., Fourgeau, I., Giard, D., 1982. Wave propagation and sampling theory. Geophysics 47, 203.

Murray, M.R., 2002. Is laser particle size determination possible for carbonate-rich lake sediments? J. Paleolimnol. 27, 173–183.

Nederbragt, A.J., Thurow, J., 2001. A 6000 year varve record of Holocene sediments in Saanich Inlet, British Columbia, from digital sediment colour analysis of ODP Leg 169S cores. Mar. Geol. 174, 95–110.

Patterson, R.T., Prokoph, A., Chang, A.S., 2004a. Late Holocene sedimentary response to solar and cosmic ray activity influenced climate variability in the NE Pacific. Sediment. Geol. 172, 67–84.

Patterson, R.T., Prokoph, A., Wright, C., Chang, A.S., Thomson, R.E., Ware, D.M., 2004b. Holocene solar variability and pelagic fish productivity in the NE Pacific. Palaeontol. Electronica 7 (4) (17 pp.).

Patterson, R.T., Prokoph, A., Kumar, A., Chang, A.S., Roe, H.M., 2005. Holocene variability in pelagic fish and phytoplankton productivity along the west coast of Vancouver Island, NE Pacific Ocean. Mar. Micropaleontol. 55, 183–204.

Pellatt, M.G., Mathewes, R.W., 1997. Holocene tree line and climate change on the Queen Charlotte Islands, Canada. Quat. Res. 48, 88–99.

Pellatt, M.G., Hebda, R.J., Mathewes, R.W., 2001. High-resolution Holocene vegetation history and climate from Hole 1034B, ODP leg 169S, Saanich Inlet, Canada. Mar. Geol. 174, 211–222.

Pickard, G.L., Stanton, B.R., 1980. Pacific Fjords — a review of their water characteristics. In: Freeland, H.J., Farmer, D.M., Levings, C.D. (Eds.), Fjord Oceanography. Plenum Press, New York, pp. 1–51.

Prokoph, A., 1999. Fractal, multifractal and sliding window correlation dimension analysis of sedimentary time series. Comput. Geosci. 25, 1009–1021.

Prokoph, A., Patterson, R.T., 2004. From depth-scale to time-scale: transforming of sediment image color data into high-resolution time-series. In: Francus, P. (Ed.), Image Analysis, Sediments and Paleoenvironments. Developments in Paleoenvironmental Research Series, vol. 7. Springer, Dordrecht, pp. 143–164. chapter 8.

Rasband, W.S., 1997. Image J. U.S. National Institute of Health, Bethesda, MA, USA. http://rsb.info.nih.gov//ij/.

Raspopov, O.M., Dergachev, V.A., Kolstroem, T., 2004. Periodicity of climate conditions and solar variability derived from dendrochronological and other palaeoclimatic data in high latitudes. Palaeogeogr. Palaeoclimatol. Palaeoecol. 209, 127–139.

Razjigaeva, N.G., Grebennikova, T.A., Ganzey, L.A., Mokhova, L.M., Bazarova, V.B., 2004. The role of global and local factors in determining the middle to late Holocene environmental history of

the South Kurile and Komandar Islands, northwestern Pacific. Palaeogeogr. Palaeoclimatol. Palaeoecol. 209, 313–333.

Rothman, D.A., Grotzinger, J.P., Flemings, P., 1994. Scaling in turbidite deposition. J. Sediment. Res., Sect. A Sediment. Pet. Proc. 64, 59–67.

Schaaf, M., Thurow, J., 1994. A fast and easy method to derive highest-resolution time-series datasets from drillcores and rock samples. Sediment. Geol. 94, 1–10.

Scherer, K., Fichtner, H., Borrmann, T., Beer, J., Desofgher, L., Flükiger, E., Fahr, H.-J., Ferreira, S.E.S., Langner, U.W., Potgieter, M.S., Heber, B., Masarik, J., Shaviv, N.J., Veizer, J., 2007. Interstellar-terrestrial relations: variable cosmic environments, the dynamic heliosphere, and their imprints on terrestrial archives and climate. Space Sci. Rev. doi:10.1007/s11214-006-9126-6.

Spooner, I.S., Barnes, S., Baltzer, K.B., Raeside, R., Osborn, G.D., Mazzucchi, D., 2002. The impact of air mass circulation dynamics on Late Holocene paleoclimate in northwestern North America. Quat. Int. 108, 77–83.

Stuiver, M., Reimer, P.J., Bard, E., Beck, J.W., Burr, G.S., Hughen, K.A., Kromer, B., McCormac, F.G., Plicht, J., Spurk, M., 1998. INTCAL 98 Radiocarbon age calibration 24,000–0 cal BP. Radiocarbon 40, 1041–1083.

Telford, R.J., Heegaard, E., Birks, H.J.B., 2004. All age–depth models are wrong: but how badly? Quat. Sci. Rev. 23, 1–5.

Thomson, R.E., 1981. Oceanography of the British Columbia coast. Can. Spec. Publ. Fish. Aquat. Sci. 56 (291 pp.).

Torrence, C., Compo, G.P., 1998. A practical guide to wavelet analysis. Bull. Am. Meteorol. Soc. 79, 61–78.

Trenbeth, K.E., Hurrell, J.W., 1994. Decadal atmosphere–ocean variations in the Pacific. Clim. Dyn. 9, 303–319.

Turcotte, D.L., Newman, W.I., 1996. Symmetries in geology and geophysics. Proc. Natl. Acad. Sci. 93, 14295–14300.

Van Hengstum, P.J., Reinhardt, E.G., Boyce, J.I., Clark, C., 2007. Changing sedimentation patterns due to historical land-use change in Frenchman's Bay, Pickering, Canada: evidence from high-resolution textural analysis. J. Paleolimnol. 37, 603–618.

Veizer, J., 2005. Celestial climate driver: a perspective from four billion years of the carbon cycle. Geosci. Can. 32, 13–30.

Ware, D.M., 1995. A century and a half of change in the climate of the NE Pacific. Fisheries Oceanogr. 4, 267–277.

Ware, D.M., Thomson, R.E., 2000. Interannual to multidecadal timescale climate variations in the Northeast Pacific. J. Climate 13, 3209–3220.

Wigston, A.P., 2006. Late Holocene Climate Change of Frederick Sound, British Columbia, Canada. Unpublished M.Sc. thesis, Carleton University.

Yu, Z., Ito, E., 1999. Possible solar forcing of century-scale drought frequency in the northern Great Plains. Geology 27, 263–266.